Journal of Applied Physics PERSPECTIVE scitation.org/journal/jap

New method enables multifunctional measurement of elastic moduli and internal frictions

Cite as: J. Appl. Phys. **128**, 230902 (2020); doi: 10.1063/5.0034801
Submitted: 23 October 2020 · Accepted: 30 November 2020 ·
Published Online: 17 December 2020

Mingyu Xie and Faxin Li[a)]

AFFILIATIONS

LTCS and Department of Mechanics and Engineering Science, College of Engineering, Peking University, Beijing 100871, China

[a)]**Author to whom correspondence should be addressed:** lifaxin@pku.edu.cn

ABSTRACT

Elastic moduli and internal frictions are fundamental properties of solid materials, and they are usually fairly sensitive to temperature, microstructure, deformation, and external fields. Measurement of elastic moduli and internal frictions is very important and useful in both academics and engineering. In this work, we first briefly reviewed the measurement methods of elastic moduli and internal frictions over the past 100 years and the related applications. Next, a promising measurement method called modified piezoelectric ultrasonic composite oscillator technique (M-PUCOT) was presented which can measure Young's modulus, shear modulus, and the related internal frictions accurately and quickly. Then, some typical measurement results using M-PUCOT on metals and phase transition materials were presented from room temperature up to 500 °C. The M-PUCOT measurement on rocks after different levels of compression was also conducted to predict the damage before fracture. The perspective and challenge of the M-PUCOT method as the indicator of heat treatment, mechanical fatigue, and early damage of metals and ceramics were further presented and discussed. It is expected that, in the near future, the measurement of elastic moduli and internal friction will be as convenient as that of electric conductivity, permittivity, etc. and can turn to be a multi-functional tool for many advanced applications.

I. INTRODUCTION AND BACKGROUND

Elastic moduli and internal frictions are the fundamental properties of solid materials. For isotropic materials, there only exist two independent elastic moduli, and Young's modulus (E) and shear modulus (G) are the most widely used. Compared with elastic moduli, internal frictions are less familiar to most readers probably because they are usually not provided in material property tables. Actually, internal frictions are usually dependent on the vibration modes,[1,2] frequency[3,4] and sometimes also dependent on the vibration amplitude[5,6] and thus cannot be treated as material constants. On the other hand, elastic moduli and internal frictions, especially the latter, are fairly sensitive to temperature, microstructure, deformation and thus can be used to monitor phase transitions of materials, sense the early damage or fatigue of components, etc.[7–9] To achieve these goals, it is necessary that the elastic moduli and internal frictions can be measured both accurately and quickly.

In the past 100 years, various measurement methods for elastic moduli and internal frictions had been developed, which can be classified into four types in terms of measurement frequency,[8] i.e., quasi-static methods, low-frequency methods, resonance methods, and ultrasonic methods. (i) The quasi-static methods measure the elastic moduli during quasi-static tensile or torsional loading[10] and measure the relaxation strength and relaxation time via strain creep[11,12] under constant stress loading or stress relaxation[13] under constant strain loading. Then, the internal friction can be calculated using the Boltzmann superposition principle.[7,9] However, the measurement errors of quasi-static methods are usually fairly large, typically larger than 10% for elastic moduli measurement and even larger for internal friction measurement. Furthermore, the quasi-static methods are rather time-consuming[14] and thus not widely used in practice. (ii) Low frequency methods drive the specimen using low frequency stimulus and measure the dynamic deformation (displacement or strain) simultaneously. Based on the amplitude and phase of the dynamic deformation, both the elastic moduli and internal frictions can be extracted. The well-known low-frequency instruments are *Kê* torsional

pendulum[15] and the commercial available dynamic mechanical analyzer (DMA).[16] The *Kê* pendulum can only measure the shear modulus and torsional internal friction using filament specimens, and the DMA are usually limited to measurement on not very hard materials such as polymers,[17] which is less accurate for metals and ceramics. (iii) Ultrasonic methods measure the ultrasonic wave velocity and attenuation on thick specimens and extract the elastic moduli and internal frictions.[18–21] Although the elastic moduli can be measured with an acceptable accuracy (~5%), the internal frictions were always overestimated because of the reflection, diffraction, and dispersion of the ultrasonic waves.[22] From the above discussions, it can be seen that none of the quasi-static methods, low-frequency methods, and ultrasonic methods can measure the elastic moduli and internal frictions accurately and quickly.

In comparison, the resonance methods can usually measure the elastic moduli and internal frictions quickly with good accuracy. The free–free beam method[23] and the impulse excitation method,[24,25] which had been chosen to be ASTM testing standard for decades, can typically measure Young's modulus and shear modulus with the testing errors within 2% and 5%, respectively. The internal frictions typically cannot be measured that accurately because the errors of the measured vibration amplitude are usually fairly large. This is caused by the fact that, to effectively excite and detect the vibration, the supporting point is usually a small distance away from the theoretical nodal position of 0.224L (L is the beam length).[7] In addition, the data fitting process of the resonance curve will introduce extra errors to the measured internal friction. However, if the specimen's resonance is excited and sensed by the contactless electrostatic[26,27] or electromagnetic acoustic transducers (EMATs),[28–30] internal frictions can also be measured very accurately using the vibration amplitude attenuation method. One problem of the electrostatic excitation method is that the excitation amplitude is too weak, especially for materials with large internal frictions.[7] Several problems exist in the EMAT method, e.g., it is only applicable to metals, its working frequency is very high (typically ~1 MHz); thus, single resonance modes are difficult to be excited, the testing setup is very complicated, etc. The resonant ultrasound spectroscopy (RUS)[30–32] method can extract all the elastic constants of anisotropic materials using regular shaped (parallelepiped or cylinder) samples. However, the difficulties of modal identification[33] and iterative convergence[34] hinder its wide use. The traditional PUCOT (piezoelectric ultrasonic composite oscillator technique) excites the specimen by using a quartz crystal bar and sense the resonance using another quartz crystal bar.[35–38] PUCOT can measure both the elastic moduli and internal friction very quickly, and automatic *in situ* measurement during heating/cooling was also realized.[39,40] However, because the piezoelectricity of the quartz crystal is rather weak, frequency match is required between the quartz crystal bar[36] and the specimen, thus the specimen's modulus should be known roughly in advance. Therefore, the traditional PUCOT was not widely used and usually employed to measure the temperature dependent internal frictions of materials with known modulus.

In the past decades, the measurement of elastic moduli and/or internal frictions had been used to study the defects dynamics, phase transitions, and degradation of materials. The common conclusion is that internal frictions are much sensitive to the microstructural change than the elastic moduli. Since 1940s, the internal frictions of metals and alloys had been intensively investigated to study the defect dynamics by physicists including Zener,[9,41,42] Snoek,[43,44] *Kê*[15,45,46] *et al.* The well-known Snoek internal friction peak was caused by interstitial atoms in body-center-cubic crystals and had been used to evaluate the carbon density in steels for over 70 yr.[43,47] The Zener internal friction peak is caused by substitutional atoms in body-center-cubic, face-center-cubic, and hexagonal crystals around 400–500 °C.[41,42] The *Kê* internal friction peak in pure polycrystalline metals (Al, Mg, Cu, etc.) was proved to be caused by the stress relaxation of grain boundaries (two-dimensional defects) and may not appear in industrial alloys.[15,46,48] The Bordoni internal friction peak appearing in face-center cubic metals was attributed to the dislocation relaxation at very low temperatures.[49–51] The internal frictions of metals were usually measured by using the *Kê* torsional pendulum[15] or Bordoni bending beam,[49] with which the shear modulus or Young's modulus can also be obtained. However, the torsional internal friction and the longitudinal/bending internal friction were not distinguished in previous studies, i.e., they are merely referred as internal frictions.

The elastic moduli and internal frictions had been used to study the phase transitions in various materials. Early in 1970, Postnikov *et al.*[52] measured the internal frictions of two types of PZT ceramics from 20 °C to 400 °C using the torsional pendulum and free–free beam resonance method. For both compositions, internal friction peaks were observed near the Curie temperature and also well below the Curie temperature. Cheng *et al.*[53–57] systematically measured Young's modulus, shear modulus, and internal frictions of $BaTiO_3$ ceramics and PZT ceramics using the free–free beam resonance method and the torsional pendulum method in a wide temperature range. They found that both elastic moduli and internal frictions appear abnormality (peaks, valleys, or inflection) near the phase transition temperature. In recent years, commercial DMA was also used to study the phase transitions in PZT and $BaTiO_3$,[58–60] and the domain evolutions under external fields were also investigated.[61,62] The torsional pendulum and DMA were also employed to study the glass transition process in bulk metallic glass.[63–65] Note that both the torsional pendulum method and the free–free beam resonance method are somewhat time-consuming, thus continuous measurement during heating/cooling is not possible. As to the DMA method, the measurement results for stiff materials are usually noisy and repeatability is typically not good.

The degradation of materials is usually accompanied by a large change of internal frictions. By using the *in situ* electromagnetic acoustic resonance technique (EMAR), Ogi *et al.* found a quick increase in the internal friction just before the fatigue failure of the 4 N polycrystalline copper[66] and carbon steel,[67] indicating that internal friction may be a useful probe to detect fatigue and damage. However, the offline measurement upon interrupting the fatigue testing of aluminum showed that the internal friction almost kept constantly before failure,[68] i.e., it cannot serve as the fatigue indicator in practice. In addition, the EMAR measured the internal frictions by using the surface shear wave attenuation, which is not sensitive to internal defects.

Recently, we proposed a modified piezoelectric ultrasonic composite oscillator technique (M-PUCOT), in which the vibration of the specimen is excited and sensed by a small piece of the PZT transducer.[69] The resonance performances of the specimen–(spacer)–transducer composite system are measured by using the susceptance curve (imaginary part of admittance), from which Young's modulus, shear modulus, and related internal frictions can be obtained via explicit formulas. This method can also be classified as a quantitative electromechanical impedance method (Q-EMI[70]) with higher accuracy, since the testing configuration is similar with the qualitative EMI method used in the field of structural health monitoring.[71,72] The measurement repeatability of M-PUCOT is very good and the measurement is very quick (~2 s), which are very convenient for continuous measurement during heating/cooling.[69] The M-PUCOT had been used to study the phase transition in soft and hard PZT ceramics (poled and unpoled),[73] which is found as convenient as the dielectric measurement. The M-PUCOT makes the measurement of elastic moduli and internal frictions a powerful tool to study phase transitions, microstructure evolutions, damage and fatigue, heat treatment, etc. in metals, ceramics, and composites.

This perspective is organized as follows. The working principle and calculation formulas of the M-PUCOT are presented in Sec. II for both the 2-component and 3-component systems. In Sec. III, various measurement results on metals, ceramics, and rocks using M-PUCOT are presented and discussed. Section IV presents the measurement repeatability and accuracy of M-PUCOT. The prospective and challenge of M-PUCOT are discussed in Sec. V. Summary and conclusion are given in Sec. VI.

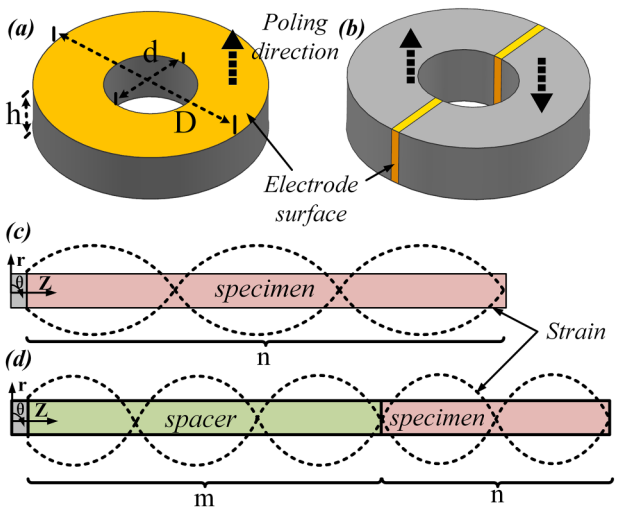

FIG. 1. Measurement principle of the M-PUCOT. (a) The d_{33} mode PZT transducer for longitudinal vibration; (b) the d_{15} mode PZT transducer for torsional vibration; (c) measurement principle for the transducer-specimen 2-component system; (Measurement principle for the transducer-spacer-specimen 3-component system. Reproduced with permission from Xie and Li, Rev. Sci. Instrum. **91**, 015110 (2020). Copyright 2020 AIP Publishing LLC.

II. THE MODIFIED PIEZOELECTRIC ULTRASONIC COMPOSITE OSCILLATOR TECHNIQUE (M-PUCOT)

In this section, the measurement principle of the M-PUCOT is first introduced, and the formulas for elastic moduli and internal frictions calculation are presented for the 2-component system and 3-component system. Then, the experimental details of M-PUCOT under room temperature and varied temperature are provided.

A. Measurement principle of M-PUCOT

As shown in Fig. 1, in M-PUCOT, we abandoned the two quartz bar oscillators in the traditional PUCOT method and replaced them with a single small PZT ring transducer (with the outer diameter D, inner diameter d, and thickness h) to both drive and gauge the vibration. For Young's modulus and longitudinal internal friction measurement, a thickness-poled d_{33}-mode PZT ring transducer with the electrodes sprayed on the upper and lower surfaces is used, as shown in Fig. 1(a); while for shear modulus and torsional internal friction measurement, the d_{15}-mode torsional transducer with two lateral electrodes is assembled by using two thickness-poled half rings with the poling direction reversed,[74] as shown in Fig. 1(b).

1. Two-component system

For measurement at room temperature, the transducer can be directly bonded onto one end of the specimen (with the diameter D), and a perfect one-dimensional longitudinal or torsional vibration can be generated by applying an AC electric field along the axial or circumferential direction of the transducer. As the thickness of the PZT transducer is much smaller than the length of the specimen, the resonance frequency of this 2-component system is very close to the specimen's own resonance frequency and is much lower than the transducer's resonance frequency. That is, compared with the traditional PUCOT that frequency match must be satisfied between the quartz crystal bar transducer and the specimen, in this M-PUCOT, no frequency match is required between the PZT transducer and the specimen. This is due to the excellent piezoelectric properties of PZT transducers, which can excite and sense the vibration far below its own resonance frequency. However, for the quartz crystal transducer used in traditional PUCOT, its piezoelectricity is rather weak and it can only work near its own resonance frequency, thus frequency match is required between the transducer and the specimen.

Unlike other resonance methods which obtain the elastic moduli and internal frictions from the resonant frequency and −3 dB points of the amplitude–frequency curves, in M-PUCOT, we only need to measure the susceptance curves (one type of the impedance curve) of the transducer–specimen composite system by using a commercial impedance analyzer. The elastic moduli and related internal frictions can be determined from the n-order resonance frequency f_n^r and anti-resonance frequency f_n^a of the slope-flattened susceptance curves.[69] The explicit formula can be derived

as follows:[69]

$$\begin{cases} E_M = \left\{\left[1+\left(1-\dfrac{d^2}{D^2}\right)\dfrac{\rho_P h}{\rho_M l_M}\right]\dfrac{f_n^{rL}+f_n^{aL}}{2}2l_M\right\}^2\dfrac{\rho_M}{n^2}, \\ G_M = \left\{\left[1+\left(1-\dfrac{d^4}{D^4}\right)\dfrac{\rho_P h}{\rho_M l_M}\right]\dfrac{f_n^{rT}+f_n^{aT}}{2}2l_M\right\}^2\dfrac{\rho_M}{n^2}, \\ Q_{ML}^{-1} = 2\dfrac{f_n^{aL}-f_n^{rL}}{f_n^{aL}+f_n^{rL}}, \\ Q_{MT}^{-1} = 2\dfrac{f_n^{aT}-f_n^{rT}}{f_n^{aT}+f_n^{rT}}, \end{cases} \quad (1)$$

where E, G, ρ, and Q^{-1} are Young's modulus, shear modulus, density, and internal friction, respectively. Subscripts "M" and "P" stand for properties of the specimen and PZT transducer, respectively. Subscripts "L" and "T" denote longitudinal and torsional vibration, respectively.

Figure 2 shows the typical susceptance curve and the amplitude–frequency curve (measured by using a laser Doppler vibrometer) of a 2-component system. It is very exciting to find that the mechanical resonance frequency f^r of the composite system is equal to $\frac{f_n^r+f_n^a}{2}$, and the resonance frequency and anti-resonance frequency of the susceptance curve coincide with the two −3 dB points of the amplitude–frequency curve. By referring to Eq. (1), the internal friction (Q^{-1}) of the composite system is expressed as $2\frac{f_n^a-f_n^r}{f_n^a+f_n^r}$, which is consistent with the universal definition of internal friction, i.e., $Q^{-1}=\Delta f/f^r$, where $\Delta f = f_n^a - f_n^r$. Due to the strain energy in the transducer is much smaller than that in the specimen, the internal friction of the PZT transducer can be neglected, which can be verified using the finite element simulations.[69]The contribution of the bonding paste can be calibrated or just neglected if measuring lossy materials ($Q^{-1} > 10^{-3}$).

2. Three-component system with frequency match

Although the 2-component system is relatively simple, it cannot be used for measurements at elevated temperatures; otherwise, the PZT transducer may be depolarized. So, for elastic moduli and internal friction measurement under varied temperature, a cylindrical thermal-insulation spacer with the same diameter D is required to insert between the transducer and the specimen, forming a 3-component system to keep the transducer working under acceptable temperatures. The spacer is usually made of fused quartz, α-alumina, or other thermal-insulation materials. It should be noted that, in the 3-component M-PUCOT system, to get the explicit formula for moduli and internal friction calculation, frequency match is required between the spacer and the specimen. In this case, there exist m and n half-wavelengths in the spacer and specimen, as that shown in Fig. 1(d). Similarly, Young's modulus (E_M), shear modulus (G_M), longitudinal internal friction (Q_{ML}^{-1}), and torsional internal frictions (Q_{MT}^{-1}) of the specimen can be expressed using explicit formulas as follows:[69]

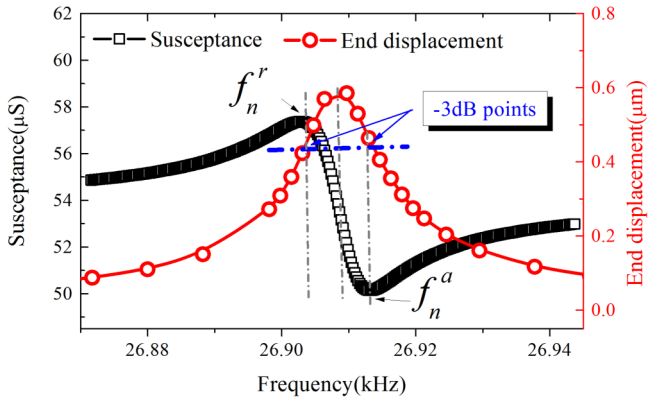

FIG. 2. Relationship between the susceptance curve and the amplitude-frequency curve in the M-PUCOT system. Reproduced with permission from Xie and Li, Rev. Sci. Instrum. **91**, 015110 (2020). Copyright 2020 AIP Publishing LLC].

$$\begin{cases} E_M = \left\{\left[1+\left(1-\dfrac{d^2}{D^2}\right)\dfrac{\rho_P h}{\rho_M l_M}+\dfrac{\rho_S l_S}{\rho_M l_M}\right]\dfrac{f_{m+n}^{rL}+f_{m+n}^{aL}}{2}2l_M-\dfrac{m\sqrt{E_S\rho_S}}{\rho_M}\right\}^2\dfrac{\rho_M}{n^2}, \\ G_M = \left\{\left[1+\left(1-\dfrac{d^4}{D^4}\right)\dfrac{\rho_P h}{\rho_M l_M}+\dfrac{\rho_S l_S}{\rho_M l_M}\right]\dfrac{f_{m+n}^{rT}+f_{m+n}^{aT}}{2}2l_M-\dfrac{m\sqrt{G_S\rho_S}}{\rho_M}\right\}^2\dfrac{\rho_M}{n^2}, \\ Q_{ML}^{-1} = 2\dfrac{f_{m+n}^{aL}-f_{m+n}^{rL}}{f_{m+n}^{aL}+f_{m+n}^{rL}}\left(1+\dfrac{m\sqrt{E_S\rho_S}}{n\sqrt{E_M\rho_M}}\right)-\dfrac{m\sqrt{E_S\rho_S}}{n\sqrt{E_M\rho_M}}Q_{SL}^{-1}, \\ Q_{MT}^{-1} = 2\dfrac{f_{m+n}^{aT}-f_{m+n}^{rT}}{f_{m+n}^{aT}+f_{m+n}^{rT}}\left(1+\dfrac{m\sqrt{G_S\rho_S}}{n\sqrt{G_M\rho_M}}\right)-\dfrac{m\sqrt{G_S\rho_S}}{n\sqrt{G_M\rho_M}}Q_{ST}^{-1}, \end{cases} \quad (2)$$

where f_{m+n}^{rL} (f_{m+n}^{rT}) and f_{m+n}^{aL} (f_{m+n}^{aT}) are $(m+n)$-order resonance frequency and anti-resonance frequency of the slope-flattening susceptance curve for longitudinal or torsional vibration, respectively. Subscripts "M," "S," and "P" stand for properties of specimen, spacer, and PZT transducer, respectively.

3. Three-component system without frequency match

The explicit formulas Eq. (1) for the 2-component system are always accuracy due to that the frequency match is not required between the PZT transducer and the specimen. However, for the

3-component system, the explicit formulas Eq. (2) are derived under the condition of frequency match between the spacer and the specimen, and the change in resonance frequency of the specimen will bring some errors in the calculation of elastic moduli and internal frictions.[75] Hence, new implicit formulas free of frequency match are also derived for the 3-component M-PUCOT. Taking the longitudinal vibration as an example, the specimen's Young's modulus and longitudinal internal friction can be expressed as[75]

$$\begin{cases} \sqrt{E_M\rho_M}\tan\left(2\pi\dfrac{f_{m+n}^{rL}+f_{m+n}^{aL}}{2}\sqrt{\dfrac{\rho_M}{E_M}}l_M\right)=C, \\ Q_{ML}^{-1}=2\dfrac{f_{m+n}^{aL}-f_{m+n}^{rL}}{f_{m+n}^{aL}+f_{m+n}^{rL}}\left(1+\dfrac{W_{SL}}{W_{ML}}\right)-\dfrac{W_{SL}}{W_{ML}}Q_{SL}^{-1}, \end{cases} \tag{3}$$

where "C" is a constant and only related to the properties of PZT transducer and spacer, $\frac{W_{SL}}{W_{ML}}$ is the strain energy ratio of the spacer and the specimen. The specific expressions of $\frac{W_{SL}}{W_{ML}}$ are shown in Ref. 75. Meanwhile, it should be noted that when the frequency match condition is satisfied, $\frac{W_{SL}}{W_{ML}}$ turns to be $\frac{m\sqrt{G_S\rho_S}}{n\sqrt{G_M\rho_M}}$ in Eq. (2). Figure 3 shows the typical calculation errors of M-PUCOT for elastic moduli and internal frictions measurement using the explicit formulas Eq. (2) and implicit formulas Eq. (3) under different levels of frequency mismatch. Meanwhile, the calculation error for internal friction measurement using traditional PUCOT is also presented for comparison. It can be seen from Fig. 3(b) that, under the same level of frequency mismatch, the internal friction calculation errors using the explicit formulas [Eq. (2)] in M-PUCOT is much smaller than that using traditional PUCOT. When the frequency mismatch is within $\pm 15\%$, the explicit formulas of M-PUCOT are suggested and the absolute errors of elastic modulus and internal friction can be within 0.5% and 2.5%, respectively. However, when the frequency mismatch is over 15%, the implicit formulas [Eq. (3)] are suggested to improve the accuracy of M-PUCOT.

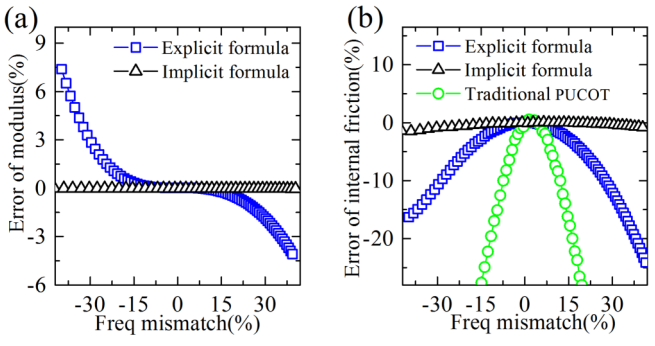

FIG. 3. Calculation errors for elastic modulus (a) and internal friction (b) measurement under longitudinal mode using explicit formulas [Eq. (2)] and implicit formulas [Eq. (3)] in M-PUCOT with different levels of frequency mismatch. Reproduced with permission from Xie and Li, Rev. Sci. Instrum. **91**, 076106 (2020). Copyright 2020 AIP Publishing LLC.

B. Experimental details

For measurement at room temperature, the transducer-specimen 2-component system and Eq. (1) are employed. Usually, the fundamental resonance mode ($n = 1$) is measured. However, for very long specimens ($l_M > 150h$), the fundamental resonance may not be detectable and higher-order resonance ($n > 1$) is suggested. The PZT transducer is bonded to the specimen using a brittle paste (502 epoxy adhesive), which can also act as an insulation layer for metal sample testing, and can be easily removed by immersing in acetone. A commercial impedance analyzer (IM3570, Japan) is used to measure the susceptance curve of the composite system. After measurement, the susceptance curve should be flattened by removing curve's slope to get the resonance peak and anti-resonance peak.[69]

For measurement under varied temperature, the specimen is put into a thermal chamber and a thermal-insulation spacer is used to form a 3-component system. In order to minimize the influence of the joint on the internal friction measurement, the length of the spacer and the specimen are carefully designed to keep the resonance anti-node at or near the joint, i.e., there exist integer half-wavelengths in each component. The fused quartz or alumina bar is suggested to serve as the spacer and high-temperature (low-temperature) ceramic paste is suggested to bond the spacer and the specimen. The choice of the spacer's material is typically based on the mismatch of the coefficient of thermal expansion (CTE) between the spacer and the specimen. According to our experiences, for specimens with low CTE (such as ceramics), a fused quartz spacer is preferred. The influence of the temperature gradient in the intermediate fused quartz spacer can be neglected because the internal frictions and frequency change (<0.3%) are very small at high temperatures.[35,36] However, for specimens with large CTE, the fused quartz spacer may break during high-temperature measurement, and the α-alumina spacer is suggested. In addition, a special metal spacer with thread is another option.

III. TYPICAL MEASUREMENT RESULTS BY USING M-PUCOT

In this section, typical testing results will be presented to show various applications of elastic modulus and internal friction measurement using M-PUCOT. First presented are the temperature dependent measurement results of structural metals with the representative of 6061Al and 314 stainless steel. Followed are the temperature dependent measurement results of phase transition materials including PZT ceramics and FeNi invar alloy. Finally, room temperature testing results on rocks after different levels of compression loading were presented to show the possibility of elastic moduli/internal frictions as the damage indicator.

A. Temperature dependent elastic moduli and internal frictions of structural metals

Structural metals such as steel, aluminum, etc. have been widely used in industries for over 100 years. The mechanical properties of structural metals at high temperatures are very important for practical applications.[76,77] For metals, it is commonly believed that the yielding stress is proportional to the elastic modulus, thus

measuring the modulus can also help to estimate the mechanical strength at high temperatures. Meanwhile, the measured internal frictions at high temperatures may provide helpful guidance for the damping design of vibrational components.

The elastic moduli and internal frictions of 6061 Al were first measured using two 10 mm-diameter, 55 mm-long cylindrical specimens, one for longitudinal mode and the other for torsional mode. For both testing, a 120 mm-long, 10 mm-diameter alumina spacer was used for thermal insulation and frequency matching. Figure 4 shows the measured susceptance curves of the transducer–spacer–6061 Al 3-component system for the longitudinal mode and torsional mode during heating from room temperature to 500 °C. It can be seen that, for both vibration modes, the measured susceptance curves are very smooth with little noise, thus the resonance peaks can be clearly determined and the obtained elastic moduli and internal frictions data are very reliable. From Fig. 4, it can be seen that the resonance frequency decreases steadily with the increasing temperature, and the resonance peaks turn from very sharp to fairly smooth at high temperatures. These results indicate that, with the increasing temperature, both Young's modulus and shear modulus of 6061 Al decrease steadily, and the internal frictions increases steadily.

Based on the measured susceptance curves in Fig. 4, Young's modulus E, shear modulus G, and the related internal frictions of 6061 Al were calculated using the explicit formula Eq. (2) and the implicit formula Eq. (3), and the results are shown in Fig. 5. At room temperature, the frequency match between the specimen and the spacer is satisfied, thus the explicit formula Eq. (2) is accurate. At high temperatures, the moduli of the specimen decreases considerably, thus the frequency match cannot be strictly satisfied and the implicit formula Eq. (3) should be more accurate. It can be seen from Fig. 5 that the obtained elastic moduli using the explicit and implicit formulas are almost the same, and both Young's modulus and shear modulus of 6061 Al decrease almost linearly with the increasing temperature. From room temperature to 500 °C, Young's modulus decreases about 27.4% from 70.3 GPa to 51 GPa, while the shear modulus decreases about 36.7% from 27.2 GPa to 17.2 GPa. The fairly large drop in elastic moduli indicates that 6061 Al is not suitable for high temperature applications around 500 °C.

It can be also seen from Fig. 5 that the obtained internal frictions (IFs) using the explicit formula is only slightly larger than that using the implicit formula at high temperatures above 450 °C, with the maximum errors no more than 5% at 500 °C. Both the longitudinal IF and the torsional IF keep almost constant (actually increase very slightly) below 300 °C, and the torsional IF is about 1.5 times of the longitudinal IF. Above 350 °C, both internal frictions increase quickly with the increasing temperature, and the torsional IF increases even faster. At 500 °C, the torsional IF reaches 13×10^{-3}, which is about 13 times of that at room temperature, while the longitudinal IF is just 7×10^{-3}, about 11 times of that at room temperature. Since even at 500 °C, when the elastic modulus decreases up to 40%, the discrepancy between the calculated internal frictions using the explicit formula and the implicit formula are no more than 5%, in the following figures, only the obtained results using the explicit formula Eq. (2) are presented.

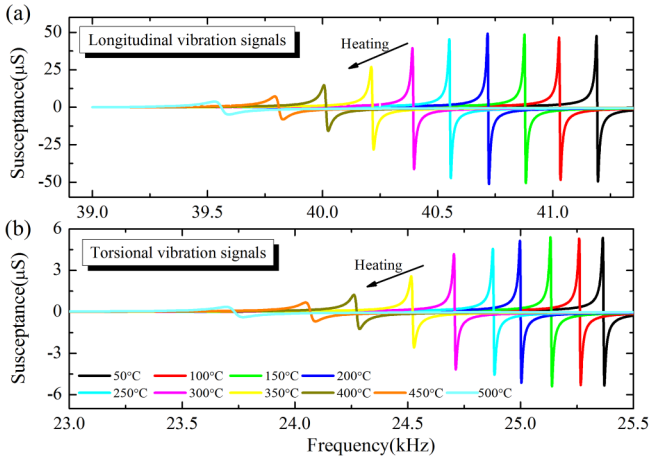

FIG. 4. Temperature dependent susceptance curves of the transducer-spacer-6061Al system. (a) Longitudinal vibration mode; (b) torsional vibration mode.

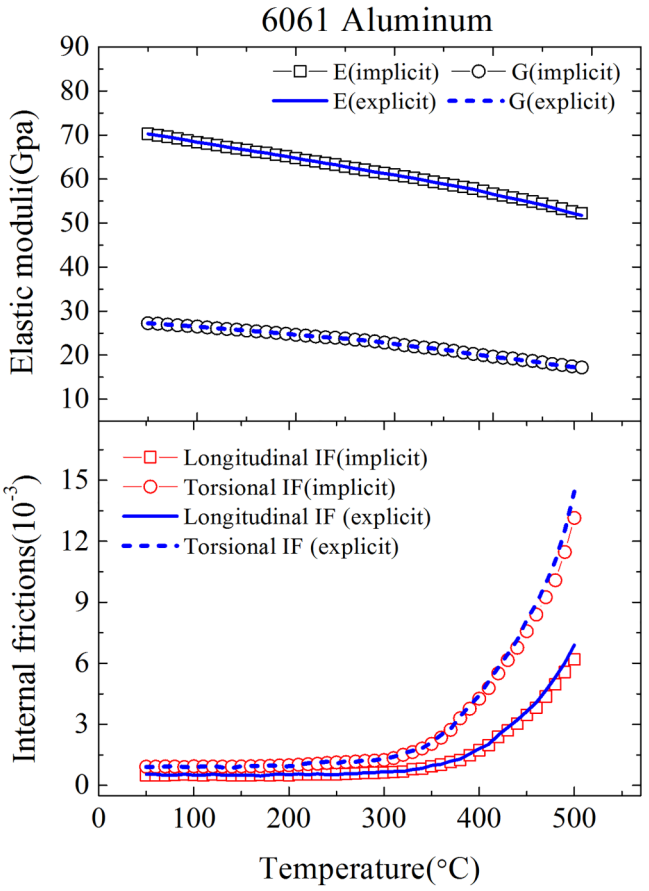

FIG. 5. Temperature dependent elastic moduli and internal frictions of 6061 aluminum using the explicit formula [Eq. (2)] and the implicit formula [Eq. (3)].

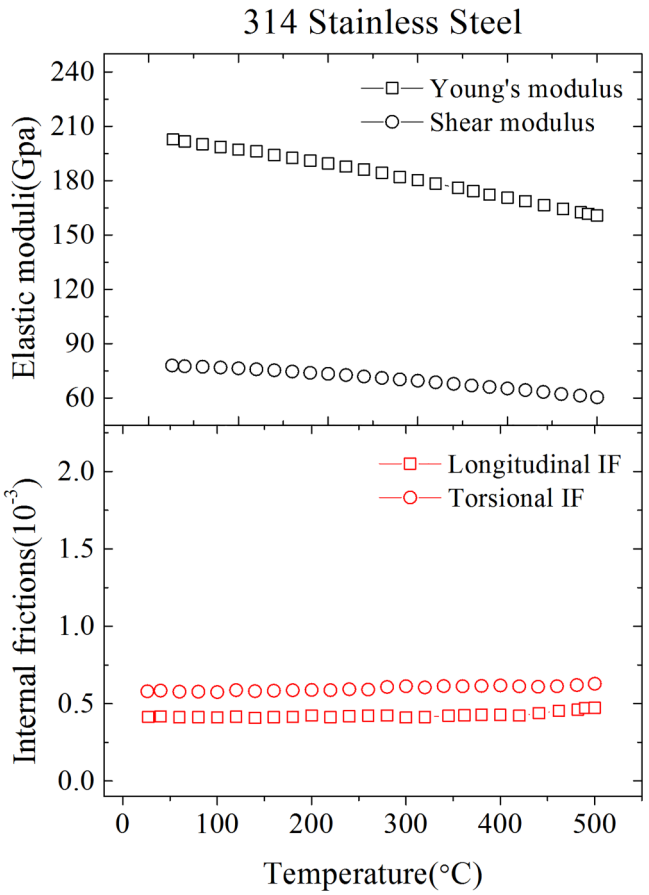

FIG. 6. Temperature dependent elastic moduli and internal frictions of 314 stainless steel.

Figure 6 shows the temperature dependent elastic moduli and internal frictions of 314 stainless steel. Similar with the case of 6061 Al, both Young's modulus and shear modulus of the steel decrease almost linearly with the increasing temperature. From room temperature to 500 °C, Young's modulus of 314 stainless steel decreases about 20% from 202 GPa to 161 GPa, and the shear modulus decreases about 22.4% from 78 GPa to 60.5 GPa. That is, the shear modulus decrease at high temperatures of 314 stainless steel is considerably smaller than that of 6061 Al, indicating that the 314 steel can still act as good structural components even at 500 °C. Different from the case in 6061 Al, both the longitudinal and torsional internal frictions (IFs) of 314 steel just increase slightly and almost linearly with the temperature. From room temperature to 500 °C, the torsional IF just increases from about 0.56×10^{-3} to 0.61×10^{-3} and the longitudinal IF only increases from 0.45×10^{-3} to 0.49×10^{-3}.

B. Variations of elastic moduli and internal frictions during phase transitions

Phase transitions in solid materials, such as ferroelectric/ferroelastic transitions,[78] martensitic transformation,[79] etc., are always accompanied by changes in elastic moduli and internal frictions, thus the measurement of elastic moduli and internal frictions can act as a useful tool to study phase transitions. In this subsection, the phase transitions in ferroelectric PZT ceramics and ferromagnetic $Fe_{64}Ni_{36}$ invar alloy were studied by the measurement of elastic moduli and internal frictions using M-PUCOT.

Figure 7 shows the measured Young's modulus, shear modulus, and related internal frictions of unpoled PZT-5A ceramics from room temperature to 600 °C. It can be seen that both elastic moduli curves and internal friction curves show inflections at the Curie temperature of 310 °C. Below that, both elastic moduli decrease slightly with the increasing temperature. However, both internal frictions firstly increase with the temperature, reaching their peaks both at about 150 °C and then decrease with the increasing temperature. Such internal friction peaks were thought to be relaxation peaks caused by domain wall motions.[58,80] In this temperature range, the torsional IF is always over twice the longitudinal IF. Above the Curie temperature of 310 °C, both Young's modulus and shear modulus first increase steadily with the increasing temperature and saturate at 165 GPa and 67 GPa, respectively,

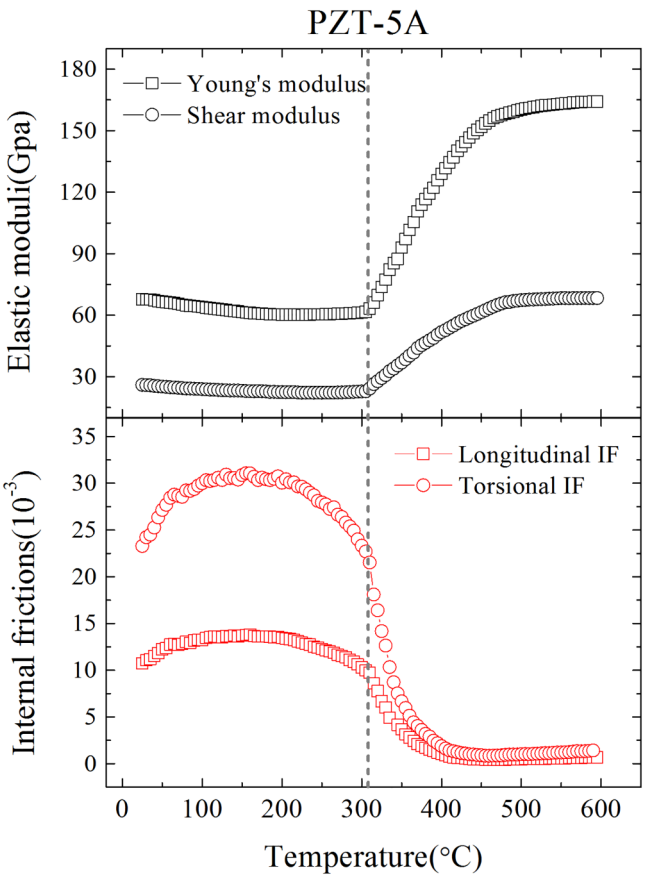

FIG. 7. Temperature dependent elastic moduli and internal frictions of PZT-5A ceramics.

above 500 °C. In comparison, both the longitudinal IF and torsional IF decrease quickly above the Curie temperature and stabilized at about 1.0×10^{-3} and 1.5×10^{-3}, respectively, above 430 °C. Note that the measured elastic moduli and internal frictions results on PZT-5A in Fig. 7 have the similar tendency as that for the PZT-5H, except that the Curie temperature is quite different, 310 °C vs 195 °C. While the measurement results on PZT-5A are quite different from those for the hard PZT-4 ceramics, although the Curie temperature is more close to each other, 310 °C vs 330 °C.[73] All these results indicate that the measurement of elastic moduli and internal frictions is a powerful tool to study phase transitions in ferroelectrics and may provide more information than the traditional dielectric measurement.

Figure 8 shows the measured elastic moduli and internal frictions of $Fe_{64}Ni_{36}$ invar alloy from room temperature to 500 °C.[69] It can be seen that both elastic moduli first increase steadily with the increasing temperature, reaching the maxima both at about 280 °C and then gradually decrease with the increasing temperature. As expected, both internal frictions first decrease steadily with the increasing temperature, reaching the minima both at about 280 °C and then gradually increase with the increasing temperature. The observed peaks in the elastic moduli curves and valleys in the internal friction curves are caused by ferromagnetic phase transitions.[81] However, the observed moduli peak (internal friction valley) temperature of 280 °C is well above the Curie temperature of about 230 °C,[82,83] which is consistent with the dilation testing results. From Fig. 8, it can also be seen that the practical resolution for the internal friction measurement is considerably better than 10^{-5}, which is very promising to detect the tiny variations in internal frictions.

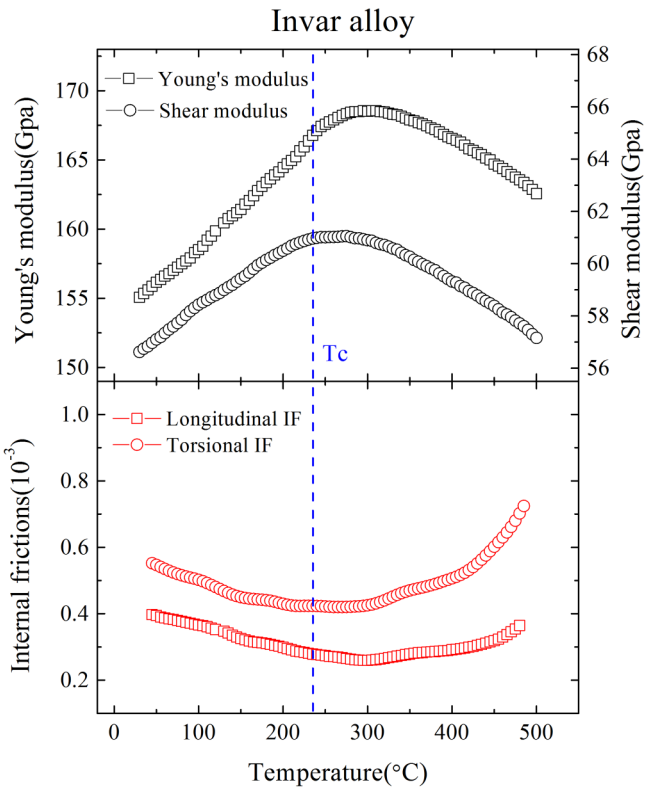

FIG. 8. Temperature dependent elastic moduli and internal frictions of $Fe_{64}Ni_{36}$ Invar alloy. [Reproduced with permission from Xie and Li, Rev. Sci. Instrum. **91**, 015110 (2020). Copyright 2020 AIP Publishing LLC].

C. Variations of elastic moduli and internal frictions after mechanical loading

For structural materials, mechanical loading may cause damage (or fatigue) inside the sample and the damage will accumulate during loading until the sample fails.[84,85] It would be very helpful if the accumulated damage before failure can be quantitatively measured or predicted. However, currently, there is no effective way to quantify the damage inside a sample. Here, we want to examine if the elastic moduli and internal frictions can be used to evaluate the damage caused by mechanical loading. The material to be tested is a brittle rock with the name of "White Jade." First, the compressive strength of the rock is measured on three cylindrical samples (with the diameter of 12 mm, length of 40 mm) by using the servo testing machine to apply the stress and using the strain gauge to record the strain. From the turning points (represents fracture) of the strain–stress curves shown in Fig. 9, it can be seen the compressive strength is between 20 and 35 MPa, with the data fairly scattered.

Then, another three White Jade rock samples were used for elastic moduli and internal frictions measurement after different levels of compression loading with the loading steps of 5–6 MPa, and the results are shown in Fig. 10. Although the measurement data are fairly scattered, some common features can be obtained from the measurement results. With the increasing compressive stress, Young's modulus ($1/S_{33}$) increases steadily or first increases then

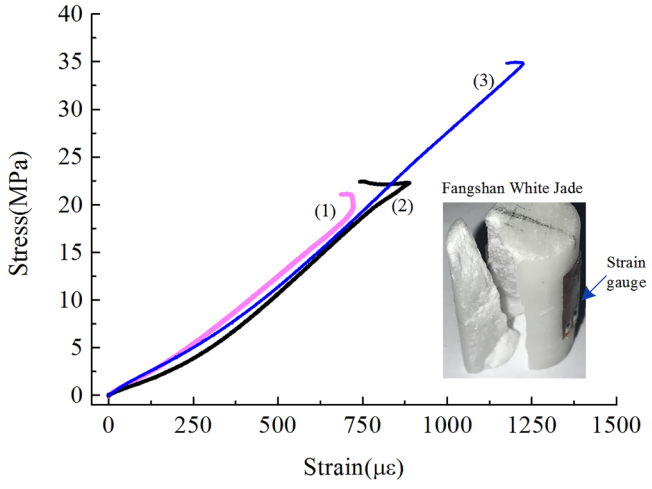

FIG. 9. Compressive strength of the White Jade rock.

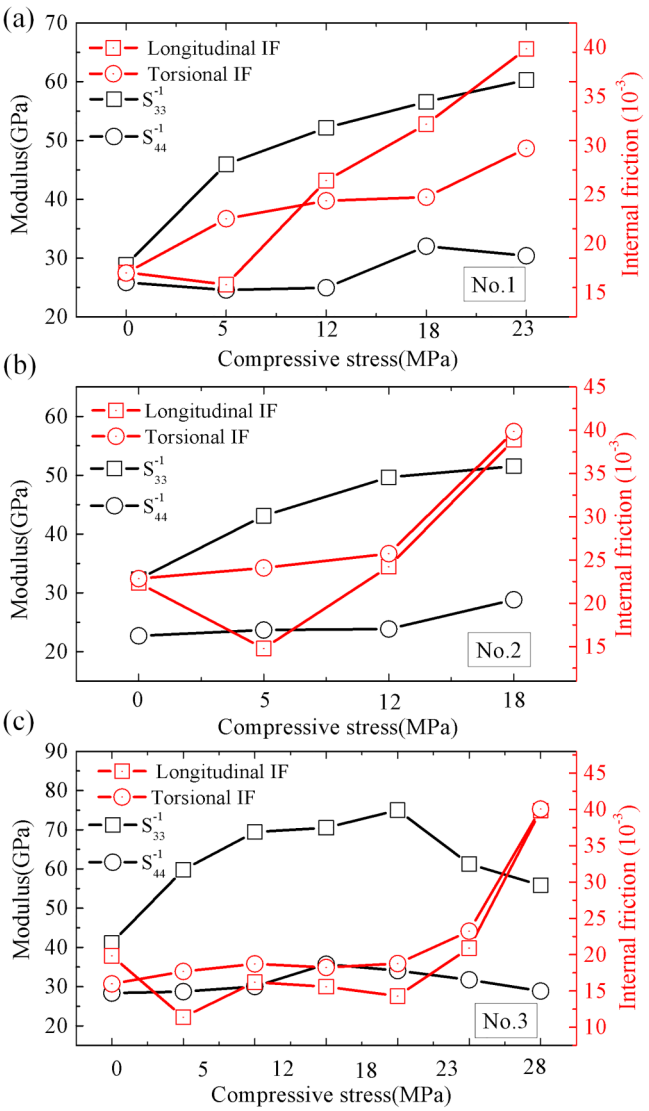

FIG. 10. Elastic moduli and internal frictions of the White Jade rocks after different levels of compressive loading. (a) No. 1 specimen; (b) No. 2 specimen; and (c) No. 3 specimen.

decreases when the stress reaches a critical value. The increase of Young's modulus is due to the decreased voids during compression, while the decrease of Young's modulus is due to the formation of microcracks inside the rock under large compressive stress. The shear modulus ($1/S_{44}$), however, almost does not change with the increasing compressive stress. The longitudinal internal friction (IF) first decreases then increases steadily when the compressive stress is larger than 5 MPa. In comparison, for all the three specimens during compression, the torsional IF increases steadily with the increasing stress. Furthermore, both internal frictions increase quickly before

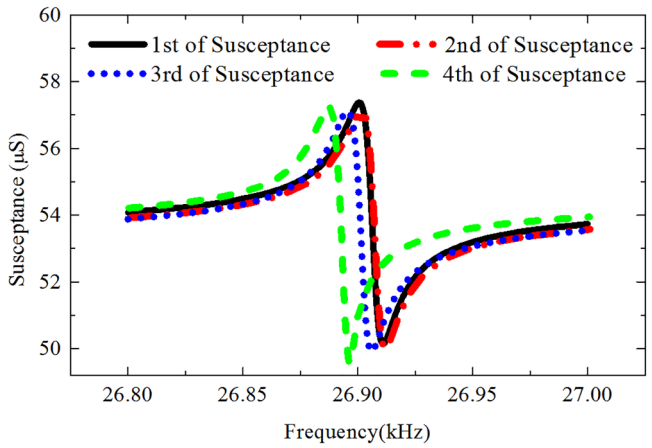

FIG. 11. Repeatability testing of the M-PUCOT 2-compoent system using the same cylindrical specimen. 1st and 2nd testing are two *in situ* measurements using Transducer A; 3rd testing is conducted after removing Transducer A and re-bonding it onto the specimen; 4th testing is conducted using another Transducer B with the same nominal parameters. [Reproduced with permission from Xie and Li, Rev. Sci. Instrum. **91**, 015110 (2020). Copyright 2020 AIP Publishing LLC.

the specimen is broken. Thus, both the longitudinal IF and torsional IF may act as early warning of rock's failure during compression.

IV. THE MEASUREMENT REPEATABLITY AND ACCRACY OF M-PUCOT

In this section, the measurement repeatability of M-PUCOT is first presented. Then, to show the accuracy of M-PUCOT, the measurement results on PZT ceramics using M-PUCOT are compared with that measured by using a commercial DMA.

A. The repeatability of M-PUCOT

Figure 11 shows the repeatability of the measurement results of M-PUCOT. It can be seen that, if using the same transducer, the repeatability error of the measured resonance frequency can be within 0.05% and that of the measured modulus is within 0.1%. For different transducers, the repeatability error of the measured modulus can be within 0.2%. It should be note that the repeatable testing errors of modulus measurement using M-PUCOT are about one order lower than the ASTM standard methods (Free-free Beam Method, ASTM 1875 and Impulse Excitation Technique, ASTM 1876), which are both about 2%.[23,24] For the measurement of internal frictions, the repeatability error is larger than that of the measured modulus, which is about 1.5% using the same transducer and about 2.5% using different transducers. This is also considerably better than the traditional vibration attenuation method, which is typically larger than 10%.[29]

B. The measurement accuracy of M-PUCOT

In order to comparatively examine the accuracy of M-PUCOT, the temperature dependent Young's modulus and internal friction

of the PZT-5H ferroelectric ceramics were measured by using the M-PUCOT and low-frequency DMA under longitudinal mode and flexural mode, respectively. The specimen used for M-PUCOT is a cylinder with the diameter of 10 mm and length of 30 mm, while the specimen used for DMA is a long strip (30 mm*6 mm*0.6 mm). From Fig. 12, it can be seen that the measured results of Young's modulus by using both methods are almost consistent, i.e., both curves show the inflection at the Curie temperature of 190 °C. Note that the measured curve using the M-PUCOT is smoother than that using DMA, indicating that M-PUCOT has smaller measurement noise. However, for the internal friction measurement, results using these two methods are quite different, although both curves show the internal friction peak at the Curie temperature of 190 °C. The internal friction measured using DMA is always considerably larger than that by using M-PUCOT, especially below the Curie temperature. This is understandable because M-PUCOT works at high frequencies (~50 kHz) and DMA works at low frequencies (0.1 Hz). The internal friction curves measured by M-PUCOT are still very smooth, while there are some abnormal fluctuations in the internal friction curves by DMA below and above the Curie temperature. The comparative measurement results indicate that M-PUCOT is obviously more accurate than DMA for measurement of "hard" materials such as ceramics and metals.

V. PERSPECTIVE AND CHALLENGE

From above, it can be seen that the M-PUCOT based measurement of elastic moduli and internal frictions is very powerful and can be widely used in a variety of fields. Besides the study of phase transitions presented in Sec. III, it can also be used to study the glass transition process in non-crystalline materials, such as bulk metallic glasses. More importantly, it can be used to study the temperature and time effect in metallurgy in a quantitative manner, i.e., monitoring the variation of elastic moduli and internal frictions, which can have great potentials in developing a precise heat treatment technique for metals and alloys. For example, the two-way shape memory effect of TiNi alloys is quite dependent on the thermal-mechanical training process, which is difficult to get the optimized performance at present. Meanwhile, the M-PUCOT can also be very useful to study the microstructure variations under an external applied field, e.g., studying the domain wall movement in ferroelectric (ferromagnetic) materials under an applied electric (magnetic) field, or under coupled thermo-electric (magnetic) loading.

Note that the internal frictions (IFs) are usually much more sensitive to microstructure variations than the elastic moduli and their measurement is independent of the specimen's size, thus the high repeatable IF measurement by using M-PUCOT is very promising in sensing the early damage and fatigue of metals, ceramics, and composites. Measurement of the amplitude dependent internal friction (ADIF) would further increase the sensitivity of IF to material degradation.[86,87] A high-voltage and high-power impedance analyzer is required to measure the impedance curve thus to get the ADIF, while currently such an impedance analyzer is not commercial available and it is under development in our group.

In this work, the testing samples are always cylinder-shaped, and the explicit formula in Eqs. (1) and (2) can be employed straightforwardly. However, in practice, the structural components

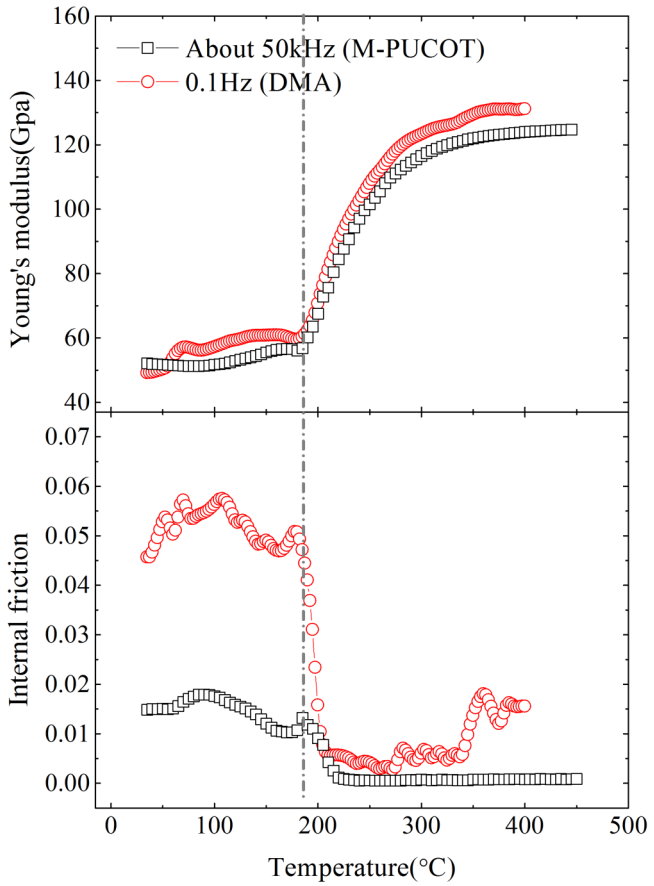

FIG. 12. The temperature-dependent Young's modulus and internal friction of the PZT-5H ferroelectric ceramics measured by using M-PUCOT and commercial dynamic mechanical analysis (DMA 242E, NETZSCH).

are usually of irregular shape. For example, the specimen for tensile loading is usually dog-bone shaped, and in this case, the formula for modulus measurement cannot be applicable any more. However, the internal friction formula in Eq. (1) can still be valid in this case, which had been verified by finite element simulations. Note that for a dog-bone shaped specimen during longitudinal or torsional resonance, the strain energy concentrated at the central thinner part, as shown in Fig. 13. In this case, the measured internal frictions are mostly determined by the central thinner part, which is very favorable to study the mechanical loading dependent internal friction evolutions in materials.

Despite the versatile functions of the measurement of elastic moduli/internal frictions using M-PUCOT, there still exist some challenges in applying this technique in some specific applications. (1) The bonding effect on the internal friction measurement. The bonding paste between the transducer, spacer, and the specimen will typically contribute to several to tens of percent of the measured internal friction, especially for metals and ceramics, whose IF are typically very small ($<10^{-4}$), although they have little

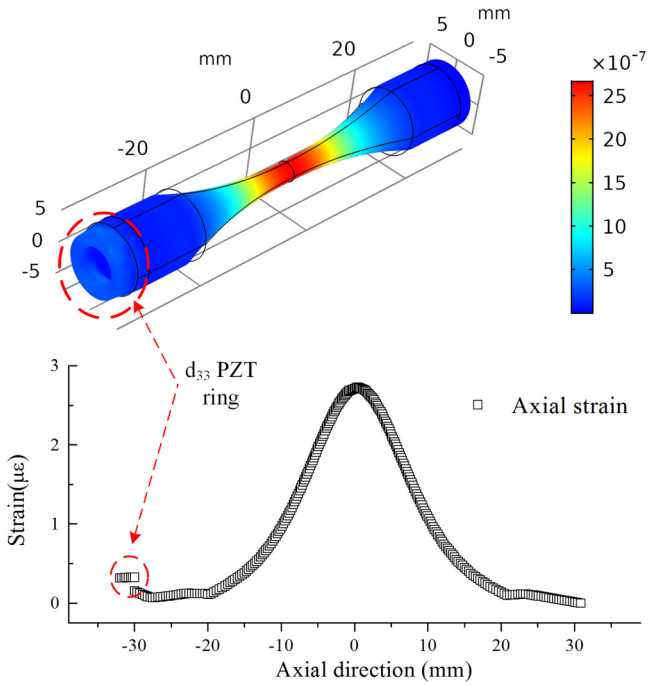

FIG. 13. Strain profile in a dog-bone shaped specimen during longitudinal resonance excited by 2 mm-thickness d33 PZT ring.

effect on the measured moduli. For measurement on metals, threaded connection can be made between the metal spacer and the specimen which can have little influence on the IF measurement. While for the lossless crystals or ceramics, the bonding effect cannot be removed as the thread connection cannot be available, thus the absolute IF is difficult to be measured very accurately. In this case, ceramic based bonding paste with very low IF is suggested and the differential method using two different-length specimens can be quite helpful.[88] (2) Measurement under very high temperatures. Theoretically, the M-PUCOT can be used at any temperature as long as the spacer is long enough for thermal insulation. However, a major problem is that large thermal stress will be generated between the spacer and the specimen, whose thermal expansion coefficients are usually different. The cost-effective quartz glass bars and alumina bars are excellent candidates for the spacer with the operating temperature typically up to 1200 °C and 1600 °C, respectively. For measurement under even higher temperatures, the high-temperature ceramic such as Si_3N_4 can be helpful. While in this case, the choice of high-temperature bonding paste turns to be another problem.

VI. CONCLUSIONS

In this Perspective, the measurement methods of elastic moduli and internal frictions were first reviewed and the related applications were discussed. Then, a promising method named M-PUCOT proposed by the authors was introduced, which can measure Young's modulus, shear modulus, and the related internal frictions quickly and with very good repeatability. Typical elastic moduli and internal friction measurement results on different materials by using M-PUCOT were presented, including the structural metals, phase transition materials, and rocks with compression damage. The prospective applications of M-PUCOT on studying the glass transition process, the temperature-time effect in metallurgy, the fatigue prediction in metals, were further discussed and the challenge of M-PUCOT in some specific applications is presented. It is expected that, by using M-PUCOT, the measurement of elastic moduli and internal frictions can be as convenient as the conductivity measurement, dielectric measurement, etc., and may turn out to be a multifunctional tool for many advanced investigations.

ACKNOWLEDGMENTS

This work was supported by the National Natural Science Foundation of China (NNSFC) under Grant No. 11890684.

DATA AVAILABILITY

The data that support the findings of this study are available from the corresponding author upon reasonable request.

REFERENCES

[1]H. Ledbetter, C. Fortunko, and P. Heyliger, J. Mater. Res. **10**, 1352 (1995).
[2]S. A. Kim and W. L. Johnson, Mater. Sci. Eng. A **452–453**, 633 (2007).
[3]T. Lee, R. S. Lakes, and A. Lal, Rev. Sci. Instrum. **71**, 2855 (2000).
[4]J. Woirgard, Y. Sarrazin, and H. Chaumet, Rev. Sci. Instrum. **48**, 1322 (1977).
[5]S. Kustov, G. Gremaud, W. Benoit, S. Golyandin, K. Sapozhnikov, Y. Nishino, and S. Asano, J. Appl. Phys. **85**, 1444 (1999).
[6]W. P. Mason, J. Acoust. Soc. Am. **28**, 1207 (1956).
[7]A. S. Nowick, *Anelastic Relaxation in Crystalline Solids* (Elsevier, 2012).
[8]M. S. Blanter, I. S. Golovin, H. Neuhauser and H.-R. Sinning, *Internal Friction in Metallic Materials: A Handbook*. Springer, Berlin Heidelberg, 1007/978 (2007).
[9]C. Zener, *Elasticity and Anelasticity of Metals* (University of Chicago Press, 1948).
[10]ASTME8/E8M-13a, *Annual Book of ASTM Standards* (ASTM International, 2001).
[11]K. Ninomiya, J. D. Ferry, and Y. Ōyanagi, J. Phys. Chem. **67**, 2297 (1963).
[12]G. B. Brook and A. H. Sully, Acta Metall. **3**, 460 (1955).
[13]S. S. Sternstein and T. C. Ho, J. Appl. Phys. **43**, 4370 (1972).
[14]G. Troxell, R. Davis and J. Raphael, *Proceedings of Proceedings ASTM* (ASTM International, 1958).
[15]T. -S. Kê, Phys. Rev. **71**, 533 (1947).
[16]E. K. Salje and W. Schranz, Z. Kristallogr. **226**, 1 (2011).
[17]Q. Li, D. Li, L.-J. Wang, N. Özkan, and Z.-H. Mao, Carbohydr. Polym. **79**, 520 (2010).
[18]J. L. Rose, *Ultrasonic Guided Waves in Solid Media* (Cambridge University Press, 2014).
[19]S. Periyannan and K. Balasubramaniam, Rev. Sci. Instrum. **86**, 114903 (2015).
[20]M. Fukuhara and I. Yamauchi, J. Mater. Sci. **28**, 4681 (1993).
[21]ASTME494-10, *Annual Book of ASTM Standards* (ASTM International, 2010).
[22]R. S. Lakes, Rev. Sci. Instrum. **75**, 797 (2004).
[23]ASTME1875-13, *Annual Book of ASTM Standards* (ASTM International, 2013).
[24]ASTME1876-15, *Annual Book of ASTM Standards* (ASTM International, 2015), Vol. 3, p. 1876
[25]G. Roebben, B. Bollen, A. Brebels, J. Van Humbeeck, and O. Van der Biest, Rev. Sci. Instrum. **68**, 4511 (1997).

[26]D. Bancroft and R. B. Jacobs, Rev. Sci. Instrum. **9**, 279 (1938).
[27]M. E. Fine, Rev. Sci. Instrum. **28**, 643 (1957).
[28]M. Hirao and H. Ogi, Ultrasonics **35**, 413 (1997).
[29]W. Johnson, B. A. Auld, and G. A. Alers, J. Acoust. Soc. Am. **95**, 1413 (1994).
[30]H. Ogi, H. Ledbetter, S. Kim, and M. Hirao, J. Acoust. Soc. Am. **106**, 660 (1999).
[31]A. Migliori, in *Resonant Ultrasound Spectroscopy* [Los Alamos National Lab.(LANL), Los Alamos, NM, 2016].
[32]R. G. Leisure and F. A. Willis, J. Phys. Condens. Matter **9**, 6001 (1997).
[33]H. Ogi, K. Sato, T. Asada, and M. Hirao, J. Acoust. Soc. Am. **112**, 2553 (2002).
[34]S. Bernard, G. Marrelec, P. Laugier, and Q. Grimal, Inverse Probl. **31**, 065010 (2015).
[35]J. Marx, Rev. Sci. Instrum. **22**, 503 (1951).
[36]W. H. Robinson and A. Edgar, IEEE Trans. Sonics Ultrason. **21**, 98 (1974).
[37]G. Gremaud, S. Kustov and O. Bremnes, in *Proceedings of Materials Science Forum* (Trans Technology Publications, 2001).
[38]W. H. Robinson, S.H. Carpenter, and J. L. Tallon, J. Appl. Phys. **45**, 1975 (1974).
[39]S. Kustov, S. Golyandin, A. Ichino, and G. Gremaud, Mater. Sci. Eng. A **442**, 532 (2006).
[40]P. M. Sutton, Phys. Rev. **91**, 816 (1953).
[41]C. Zener, Trans. AIME **152**, 122 (1943).
[42]C. Zener, Phys. Rev. **71**, 34 (1947).
[43]J. Snoek, Physica **8**, 711 (1941).
[44]J. L. Snoek, Physica **14**, 207 (1948).
[45]T. S. Kê, J. Appl. Phys. **20**, 274 (1949).
[46]T. S. Kê, J. Appl. Phys. **21**, 414 (1950).
[47]H. Saitoh, N. Yoshinaga, and K. Ushioda, Acta Mater. **52**, 1255 (2004).
[48]T. Kê and R. F. Mehl, Metall. Mater. Trans. A **30**, 2267 (1999).
[49]P. G. Bordoni, J. Acoust. Soc. Am. **26**, 495 (1954).
[50]D. H. Niblett and J. Wilks, Adv. Phys. **9**, 1 (1960).
[51]G. Fantozzi, C. Esnouf, W. Benoit, and I. G. Ritchie, Prog. Mater. Sci. **27**, 311 (1982).
[52]V. S. Postnikov, V. S. Pavlov, and S. K. Turkov, J. Phys. Chem. Solids **31**, 1785 (1970).
[53]B. L. Cheng, M. Gabbay, and G. Fantozzi, J. Mater. Sci. **31**, 4141 (1996).
[54]B. L. Cheng, M. Gabbay, G. Fantozzi, and W. Duffy, Jr., J. Alloys Compd. **211–212**, 352 (1994).
[55]B. Cheng, M. Gabbay, and G. Fantozzi, *M3D III: Mechanics and Mechanisms of Material Damping* (ASTM International, 1997).
[56]E. M. Bourim, H. Tanaka, M. Gabbay, G. Fantozzi, and B. L. Cheng, J. Appl. Phys. **91**, 6662 (2002).
[57]H. Frayssignes, M. Gabbay, G. Fantozzi, N. Porch, B. L. Cheng, and T. W. Button, J. Eur. Ceram. Soc. **24**, 2989 (2004).
[58]C. Wu, X. Wang, and X. Yao, Ceram. Int. **38**, S13 (2012).
[59]Y. Yu, H. Zou, Q.-F. Cao, X.-S. Wang, Y.-X. Li, and X. Yao, Ferroelectrics **487**, 77 (2015).
[60]C. Wang, S. A. T. Redfern, M. Daraktchiev, and R. J. Harrison, Appl. Phys. Lett. **89**, 152906 (2006).
[61]B. Jiménez and J. M. Vicente, J. Phys. D Appl. Phys. **33**, 1525 (2000).
[62]V. Ryzhenko, L. Burianova, and P. Hana, J. Electroceram. **20**, 35 (2008).
[63]J. C. Qiao and J.-M. Pelletier, J. Alloys Compd. **589**, 263 (2014).
[64]H.-R. Sinning and F. Haessner, J. Non-Cryst. Solids **93**, 53 (1987).
[65]J. C. Qiao and J.-M. Pelletier, J. Mater. Sci. Technol. **30**, 523 (2014).
[66]M. Hirao, H. Ogi, N. Suzuki, and T. Ohtani, Acta Mater. **48**, 517 (2000).
[67]H. Ogi, M. Hirao, and S. Aoki, J. Appl. Phys. **90**, 438 (2001).
[68]H. Ogi, T. Hamaguchi, and M. Hirao, Metall. Mater. Trans. A **31**, 1121 (2000).
[69]M. Xie and F. Li, Rev. Sci. Instrum. **91**, 015110 (2020).
[70]J. Fu, C. Tan, and F. Li, Smart Mater. Struct. **24**, 065038 (2015).
[71]W. Na and J. Baek, Sensors **18**, 1307 (2018).
[72]V. G. M. Annamdas and C. K. Soh, J. Intell. Mater. Syst. Struct. **21**, 41 (2010).
[73]M. Xie and F. Li, AIP Adv. **10**, 045007 (2020).
[74]M. Xie, Q. Huan, and F. Li, Ultrasonics **103**, 106101 (2020).
[75]M. Xie and F. Li, Rev. Sci. Instrum. **91**, 076106 (2020).
[76]D. Gerlich and E. S. Fisher, J. Phys. Chem. Solids **30**, 1197 (1969).
[77]W.-Y. Wang, B. Liu, and V. Kodur, J. Mater. Civ. Eng. **25**, 174 (2013).
[78]W. Yening, S. Wenyuan, C. Xiaohua, S. Huimin, and L. Baosheng, Phys. Status Solidi A **102**, 279 (1987).
[79]I. Yoshida, T. Ono, and M. Asai, J. Alloys Compd. **310**, 339 (2000).
[80]M. Daraktchiev, R. J. Harrison, E. H. Mountstevens, and S. A. T. Redfern, Mater. Sci. Eng. A **442**, 199 (2006).
[81]A. V. Deryabin, V. K. Kazantsev, and B. N. Shvetsov, J. Magn. Magn. Mater. **51**, 98 (1985).
[82]Y. Tanji, Y. Shirakawa, and H. Moriya, Sci. Rep. Res. Inst. Tohoku Univ. Ser. A Phys. Chem. Metall. **22**, 84 (1970).
[83]T. Maeda, J. Phys. Soc. Jpn. **30**, 375 (1971).
[84]M. Mehdizadeh and M. M. Khonsari, Int. J. Fatigue **114**, 159 (2018).
[85]S. M. McGuire, M. E. Fine, O. Buck, and J. D. Achenbach, J. Mater. Res. **8**, 2216 (1993).
[86]W. P. Mason, Eng. Fract. Mech. **8**, 89 (1976).
[87]H. Kousek, P. Bajons, and H. Müllner, Phys. Status Solidi A **38**, 199 (1976).
[88]J. Marx and J. Sivertsen, J. Appl. Phys. **24**, 81 (1953).